PRELIMINARY CONCEPTUAL AEROELASTIC DESIGN

Jean-Michel Dhainaut
Embry-Riddle University
Daytona Beach, FL 32114

ABSTRACT

The purpose of this paper was to develop a computer program for the preliminary design of wings and empennages at any flight regime for transport aircraft. Starting from a reduced geometry, material and aerodynamic data the flutter boundaries were accurately predicted, and the basic layout of the structure designed. The program was developed in Matlab with integrated data used for corrections of the bending frequency due to the sweep angle, and the flutter velocity due to compressibility effects at high Mach numbers. The procedure exposed could be applied towards the certification and the development of scale prototype demonstrating key design and technological aspects. This program could be used by the private sector in order to reduce risks in developing reliable vehicles, and by student as a preliminary aircraft design tool. Results include a sample of the Matlab input file, flutter boundaries at different altitudes, and some design figures changing structural and aerodynamic parameters are also addressed.

INTRODUCTION

Since the beginning of modern aviation, engineers have been designing faster aircraft, and have constantly been pushing the limits of new available technologies. Many are now working to push the speed envelope to the next great frontier, that of hypersonic speed. From the classic design of the first aircraft to the more futuristic design of the *Waverider* (X-43) that uses its own shock wave to improve its overall performance, all need wings and empennages to assure stability and maneuvering during flight. At the early conceptual design stage it is often necessary to obtain initial estimates for divergence and flutter, when only the basic geometry of the wing/tail surface are known, and much of the structural and aerodynamic properties are yet to be established[1]. Parametric studies to determine the effect of varying some of the structural-aerodynamic variables on the flutter instability boundary are convenient. The selected approach for the parametric studies was the *conceptual analysis* that is comprehensive and widely used in the aeroelasticity community. Generally speaking, *conceptual flutter analysis* has been proven extremely successful in the last decades. Disagreement between calculated flutter speed and experimental value is attributed to poor aerodynamic assumptions. The discrepancy between theoretical and experimental values is primarily due to the compressibility effect that is extremely hard to include in present aeroelastic formulations. Depending on the applications, one theory may have advantages over another. The author decided to select simpler, more readily available, approximate

Copyright @ 2005, American Society of Engineering Education

solutions for analysis of these flows for high aspect ratio wings/tails. For subsonic flows the well-defined thin-airfoil theory was selected. However, transonic, supersonic and hypersonic aerodynamics are difficult and complex fields that are still dominated by the power of Computational Fluid Dynamics (CFD) and experimental data. For supersonic compressible flows the method chosen was the *Prandtl-Glauert*, while for hypersonic flows the *Newtonian* flow theory published in his *Principia* in 1687 was preferred[2].

Currently, flutter problems at high subsonic, transonic, and supersonic flight regimes are encountered more often in non-military aircraft. The *preliminary conceptual wing flutter design* software could also be used for certification of aircraft under part 23 (transport aircraft) or part 25 (small aircraft) of the airworthiness standards of the Federal Administration Regulations (FAR).

APPROACH

Theoretical Background

As a concrete example to define the selected approach, let select a swept cantilever wing while an airstream flows over it (Fig.1). The elastic axis, assumed to be a straight line, is chosen as the reference line for measuring wing deformations.

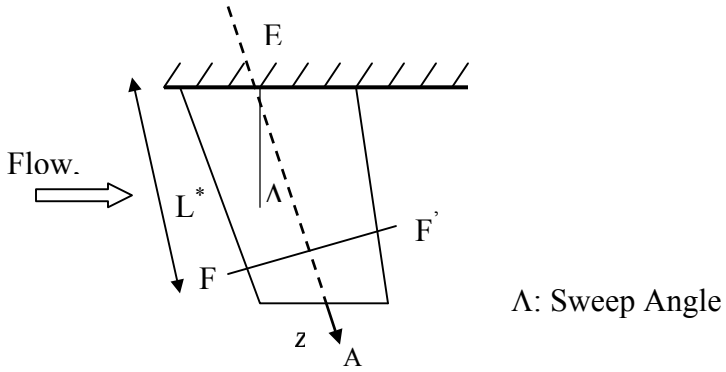

Figure. 1. Swept Cantilever Wing

The wing/tail deformation in the chordwise direction is described by two quantities: the bending and the pitch about the elastic axis. At a spanwise coordinate location *z*, and at time *t*, the bending and pitch are denoted by a complete set of generalized coordinates, $h(z,t) = b_0 \phi_h(z) q_h(t)$, and $\alpha(z,t) = \phi_\alpha(z) q_\alpha(t)$, respectively. These functions are called modes of deformations or simply mode shapes. If the functions $\phi_h(z)$ and $\phi_\alpha(z)$ are conveniently chosen, a good approximation of the divergence and flutter speed is obtained. Generally, the functions $\phi_h(z)$ and $\phi_\alpha(z)$ may be chosen as the uncoupled modes of vibration. However, better results can be obtained by using the normal modes of free vibration of the wing. For ease of computation, they may also be chosen as polynomials or other elementary functions approximating the uncoupled vibration modes[3]. In addition, the assumed functions must satisfy the geometric boundary conditions imposed upon the system. As examples, the following sets of function may

Copyright @ 2005, American Society of Engineering Education

give a fair representation of a swept cantilever wing, $\phi_h(z) = (z/L)^2$ and $\phi_\alpha(z) = z/L$. By selecting these functions, it is assumed that the total bending deformation is defined by $(z/L)^2$, and the total pitch deformation by z/L only. However, more than one mode shape can be considered to define the deformations, and the expression become lengthier. For instance, the three modes solution for the bending will be of the form

$$h(z,t) = b_0 \{\phi_{h1}(z)\, q_{h1}(t) + \phi_{h2}(z)\, q_{h2}(t) + \phi_{h3}(z)\, q_{h3}(t)\} \tag{1}$$

where $\phi_{h1}(z)$, $\phi_{h2}(z)$, and $\phi_{h3}(z)$ are modes of deformation. A comparison of flutter speed obtained by using different number of modes (n=1,2…) of deformation will give some indication of the degree of accuracy achieved. In this paper, two-degree of freedom (bending, pitch) are selected because they provides a system, which is not only easily evaluated in physical terms but also from the computational point of view. Finally, the two-degree of freedom equations of motion can be derived using the Lagrange's principle yielding to,

$$\begin{bmatrix} M_{hh} b_0 & M_{h\alpha} b_0 \\ M_{\alpha h} b_0 & M_{\alpha\alpha} \end{bmatrix} \begin{Bmatrix} \ddot{q}_h \\ \ddot{q}_\alpha \end{Bmatrix} \\ \ldots + \begin{bmatrix} \omega_h^2 M_{hh} b_0^2 - q A_{hh} b_0^2 & -q A_{h\alpha} b_0 \\ -q A_{\alpha h}.b_0 & \omega_\alpha^2 M_{\alpha\alpha} - q A_{\alpha\alpha} \end{bmatrix} \begin{Bmatrix} q_h \\ q_\alpha \end{Bmatrix} = \begin{Bmatrix} 0 \\ 0 \end{Bmatrix} \tag{2}$$

where M_{hh}, $M_{h\alpha}$, $M_{\alpha h}$, $M_{\alpha\alpha}$ and A_{hh}, $A_{h\alpha}$, $A_{\alpha h}$, $A_{\alpha\alpha}$ are generalized mass and aerodynamic terms, respectively. The uncoupled bending frequency is estimated using Galerkin's approach, and the torsional frequency is derived as shown in the Appendix. For simplicity in notation, the equations of motion are rewritten as

$$([M]\{\ddot{q}\} + [K - qA])\{q\} = \{0\} \tag{3}$$

Solution Procedure

Assuming harmonic solution of the form $\{q\} = \{q_0\} e^{i\omega t}$, and substituting into (3), the equations of motion become $(-\omega^2[M] + [K - qA])\{q_0\} e^{i\omega t} = \{0\}$, where the matrix $[K - qA]$ is in function of the dynamic pressure, q. For a given dynamic pressure the stability behavior of the system is studied by solving the eigenvalue problem. As the dynamic pressure increases, the eigenvalues ($\lambda=\omega^2$) of the different modes merge to a complex conjugate pair that leads to an unstable system. The real part of the complex conjugate is the uncoupled flutter frequency, while the imaginary part is the structural damping ratio. The transition from stable to unstable system defines the flutter boundary. Figure 2 shows a typical flutter stability curve for a two-degree of freedom system where the critical flutter frequency is always between the bending and torsional frequencies.

Copyright @ 2005, American Society of Engineering Education

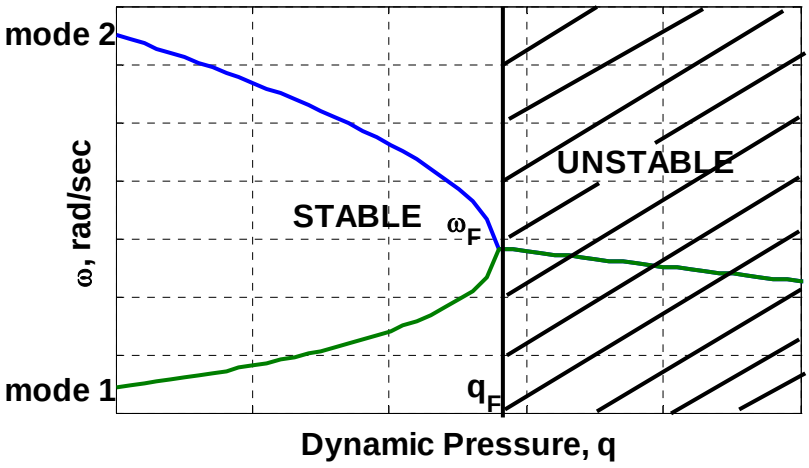

Figure. 2. Flutter Analysis for Two Modes

Wing/Tail Box Structure

The beam section with skin thickness $\bar{t}$ is shown in fig.3. Assuming thin-walled structure and neglecting higher powers of $\bar{t}$ in the computation of the sectional properties, the moment of inertia I_{xx} is approximated by $I_{xx} \approx \bar{t}\,\bar{h}^2/6(\bar{a}+\bar{b})$. Combining this equation with the calculation of the bending frequency a close-form expression for the thickness is found, $\bar{t} \approx 6\omega_F^2 M^* L^{*4}/\bar{h}^2(\bar{a}+\bar{b})C_n^2 E$.

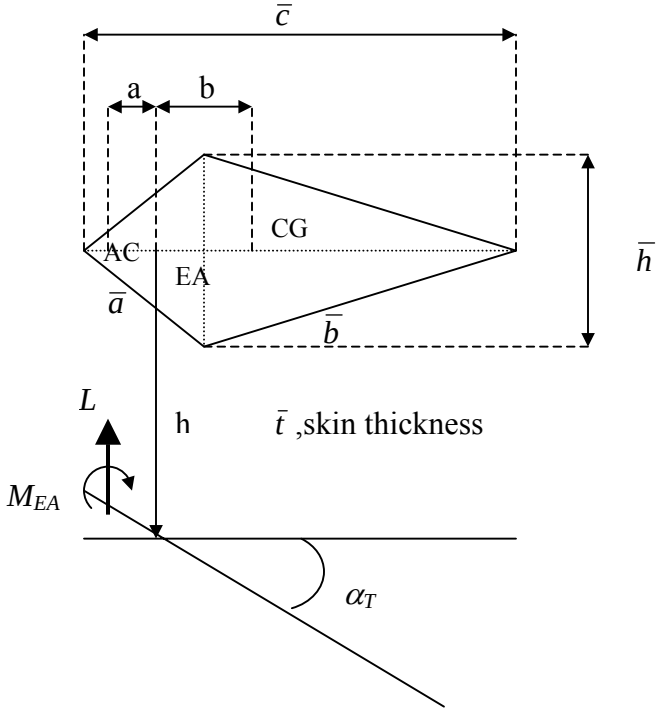

Figure. 3. Airfoil Cross-Section

Copyright @ 2005, American Society of Engineering Education

RESULTS AND DISCUSSION

The software for *Conceptual Wing Flutter Design* was verified with experimental and analytical data contained in Ref.[4]. Results include parametric study of the variation of the flutter boundary with altitude, frequency, and Young's modulus. Thickness of the wing/tail box structure for different materials is also addressed. The use of the Software does not require a thorough knowledge about aeroelasticity, and it can furnish readily available divergence/flutter results to novel engineer and students. The Software is run on a PC with Intel® Pentium, 1M RAM and maximum running time never exceeded ten minutes.

Sample Matlab input file,

```
clear;clc
format short
% main Input File
% ---- Geometric Input
L=106.8;                    % Length of Wing Platform, ft
cr=35.4;                    % Chord Length, ft
lambda=0.41;                % Wing Taper ratio
x_ac=0.25;                  % Position of Aerodynamic center (A.C) in Percentage of Chord
length
x_ea=0.35;                  % Position of Elastic Axis (E.A) in Percentage of Chord length
x_cg=0.45;                  % Position of center of gravity (C.G) in Percentage of Chord
length
Lambda=24;                  % Sweep Angle in Degrees
% ---- Mass/Material Input
m_wing=2500;                % Mass of One Side of the Wing Platform, lb

E=10.5E6;                   % Bending Modulus of Elasticity (Young's Modulus), psi

% ---- Aerodynamics Input

AR=L/2/cr/(1+lambda);       % Aspect Ratio
C_L_alpha=4.8;              % Wing Lift Coefficient per slope

% ---- Miscelaneous Data
pi=3.14159;
Lambda=pi/180*Lambda;
```

Figure 4 shows the variation on the flutter boundary at different altitudes. It is observed that at higher altitudes the Mach number at which flutter occurs increases. This is due to the fact that air density decreases with altitude, and consequently the lift force also decreases since it is in function of the dynamic pressure *q*, which is directly proportional to the air density. The air becoming less dense the action of the lift force diminishes, increasing the flutter speed. The calculated divergence Mach number for each of the altitudes, sea level, 10K ft, 55K ft, are 2.0, 2.4, and 3.4, respectively.

The next three figures could be used as parametric curves to define preliminary aircarft design guidelines.

Copyright @ 2005, American Society of Engineering Education

Figure 5 represents the flutter frequency with its corresponding Mach number for five different materials (wood, aluminum, titanium, steel and kevlar) at 10,000 feet. These curves could help design engineers and students to select the most adequate material for the required mission profile. For instance, suppose that one design requirement is to have a cruising speed of M=0.6. Looking at the curve for M=0.6 it is noticed that in order for the wing section to be stable either aluminum, steel, titanium or Kevlar could be used. This figure becomes more practical for detail analysis of control surfaces where localized flutter phenomena may be encountered. For instance, if an aluminum aileron has flutter issues at a speed of M=0.6, the problem could be solved easily by just replacing it by a composite one (Kevlar) with M=1.3. Figure 5 can also be used to see what is the maximum Mach number for different materials having different modulus of elasticity E.

Finally, Figure 6 shows the thickness of a tail/wing box structure with consequent modulus of elasticity and Mach number. This figure could be used for preliminary material and wing/tail box thickness selection at a specified Mach number for a fixed structural weight. It is interesting to notice, as it is the case in almost all aircraft, that the aluminum is the material that allows the thinner thickness, and covers Mach ranges used by general, commercial, and military aviation.

Figures 4 to 6 have been obtained by just varying the input diameters in the input file given at the beginning of this section. Other interesting design figures could be obtained by varying different parameters. For instance, the variation of the flutter speed with respect to varying lift curve slope coefficient ($C_{L\alpha}$) could be studied. That would be similar to study flutter at different flight phases (take-off, cruise, landing) or for different airfoils geometries.

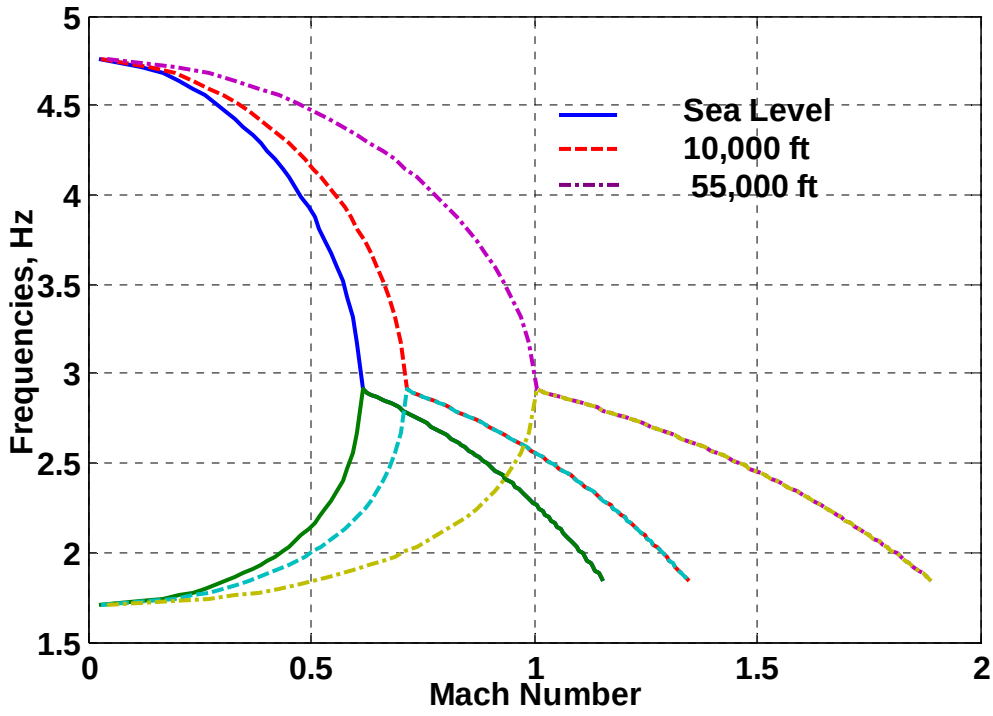

Figure. 4. Flutter Boundaries at Sea Level, 10,000 ft, and 55,000 ft

Copyright @ 2005, American Society of Engineering Education

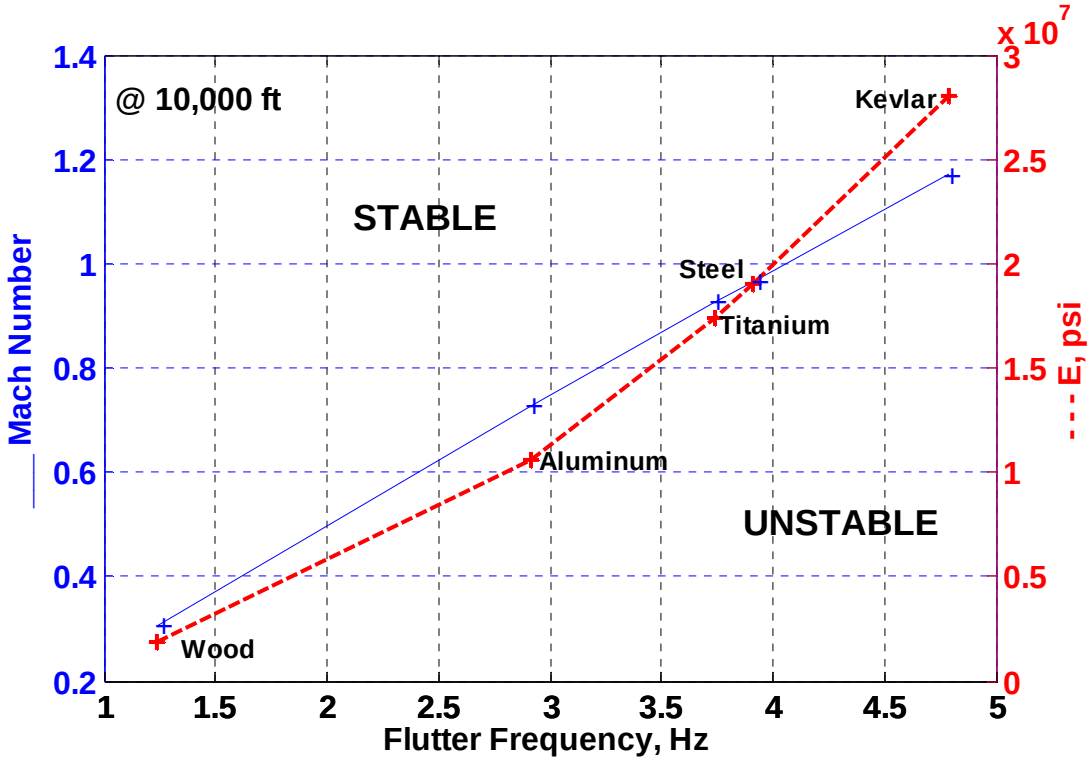

Figure. 5. Flutter Frequency Vs. Mach Number and Young's Modulus

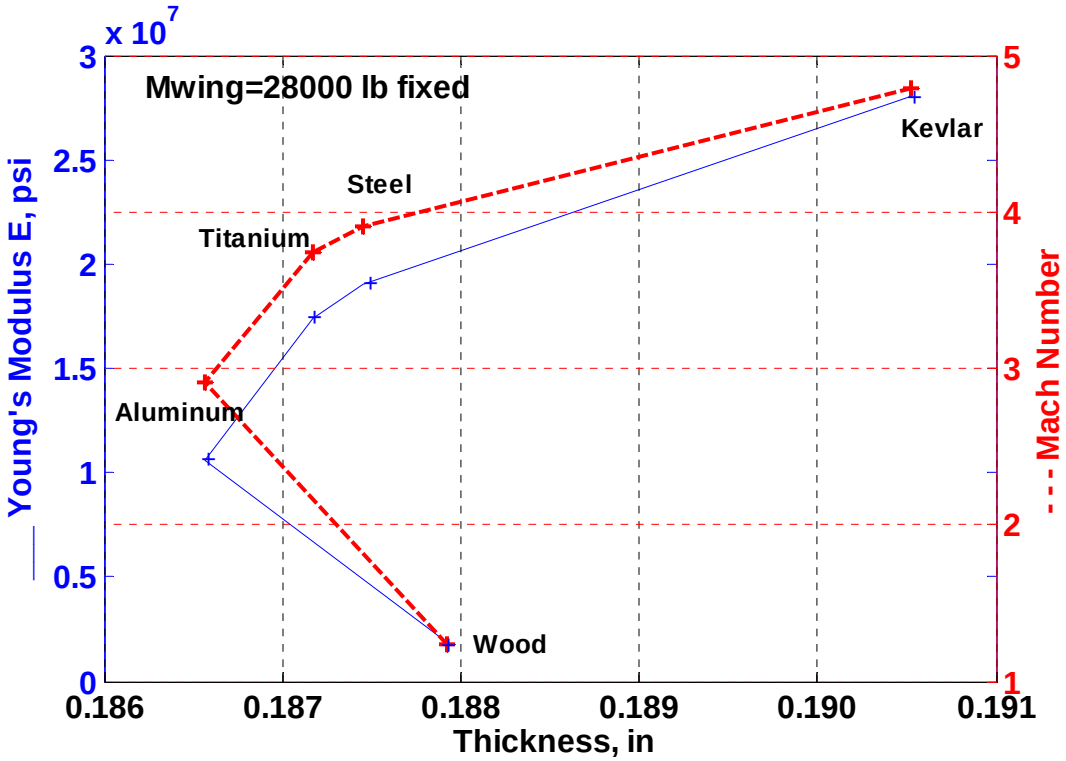

Figure. 6. Thickness Vs. Young Modulus and Mach Number

Copyright @ 2005, American Society of Engineering Education

CONCLUSIONS

A friendly interactive computer program for quick preliminary flutter analysis of wing/tail structures was developed using Matlab. The analysis was based on *Conceptual Analysis*, and different aerodynamic theories where considered, depending on the Mach number. The conceptual flutter analysis was proven accurate for subsonic (M<0.85) flight regimes where benchmark results were readily available. Lack of data for flight regimes higher than M=0.85 did not permit reliable comparison. The Software presented herein is friendly user, and yield to accurate results for preliminary flutter design consideration of wings and control surfaces. The Software could also be used to generate design curves by varying different material and aerodynamic parameters.

REFERENCES

1. V. Mukhopadhyay, "Interactive Flutter Analysis and Parametric Study for Conceptual Wing Design," AIAA 95-3943, Los Angeles, CA.
2. J. D. Anderson, Jr., "A Survey of Modern Research in Hypersonic Aerodynamics," AIAA, 17th Fluid Dynamics, Plasma Dynamics, and Lasers Conference, Snowmass, CO, 1984.
3. Y. C. Fung, *An Introduction to the Theory of Aeroelasticity*, Dover Publication, New York, 1969.
4. J. M. Dhainaut and M. A. Ferman, "Experiences with the design, Fabrication and Testing of a Scaled Flutter Model of a Large Transport Wing in the Parks College Wind Tunnel," ASEE Conference, Oshkosh, July 1999.

BIOGRAPHY

JEAN-MICHEL DHAINAUT is an assistant professor at the engineering science department of Embry-Riddle Aeronautical University, Daytona Beach campus.

APPENDIX

Mass terms:

$$M_{hh} = \int_0^{L^*} \overline{m}.\phi_h^2 dz$$

$$M_{h\alpha} = M_{\alpha h} = \int_0^{L^*} \overline{m}.b.\phi_h.\phi_\alpha dz$$

$$M_{\alpha\alpha} = \int_0^{L^*} \left(\overline{I}_{CG} + \overline{m}.b^2\right)\phi_\alpha^2 dz$$

Aerodynamic terms:

$$A_{hh} = -C_{L\alpha}\int_0^{L^*} \overline{c}\left[\phi_h.\frac{\partial\phi_h}{\partial z}.\sin\Lambda - a.\left(\frac{\partial\phi_h}{\partial z}\right)^2.\sin^2\Lambda\right]dz$$

$$A_{h\alpha} = -C_{L\alpha}\int_0^{L^*} \overline{c}\left[\phi_h.\phi_h.\cos\Lambda - a.\frac{\partial\phi_h}{\partial z}.\sin\Lambda.\cos\Lambda\right]dz$$

Copyright @ 2005, American Society of Engineering Education

$$A_{\alpha h} = C_{L\alpha} \int_0^{L^*} \bar{c} \left[a . \frac{\partial \phi_h}{\partial z} . \sin \Lambda . \cos \Lambda \right] dz$$

$$A_{\alpha\alpha} = C_{L\alpha} \int_0^{L^*} \bar{c} . \left[a . \phi_\alpha^2 . \cos^2 \Lambda \right] dz$$

Estimation of Torsional Rigidity:

From classic beam theory, the moment and torque are equal to

$$M = EI . \frac{d^2 w}{dz^2} \quad \text{(A1)}$$

$$T = GJ . \frac{d\theta}{dz} \quad \text{(A2)}$$

Dividing (A2) by (A1),

$$\frac{T}{M} = \frac{GJ}{b_0 . EI} . \frac{d\phi_\alpha / dz}{d^2 \phi_h / dz^2} \quad \text{(A3)}$$

The moment and torque are approximated by,

$$T = L.a \quad \text{(A4)}$$

$$M = L.d \quad \text{(A5)}$$

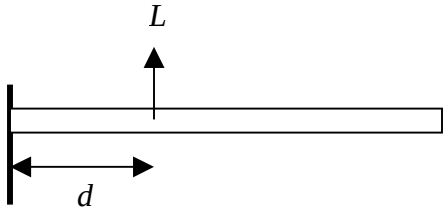

Substituting (A4) and (A5) into (A3),

$$\frac{T}{M} = \frac{L.a}{L.d} \frac{GJ}{b_0 . EI} . \frac{d\phi_\alpha / dz}{d^2 \phi_h / dz^2}$$

$$\Rightarrow GJ = \frac{b_0 . a . EI}{d} . \frac{d\phi_\alpha / dz}{d^2 \phi_h / dz^2} \quad \text{(A6)}$$

Copyright @ 2005, American Society of Engineering Education